Journal of Innate Immunity

Research Article

J Innate Immun 2022;14:243–256
DOI: 10.1159/000519305

Received: February 21, 2021
Accepted: August 30, 2021
Published online: October 20, 2021

The Gene Signature of Activated M-CSF-Primed Human Monocyte-Derived Macrophages Is IL-10-Dependent

Víctor D. Cuevas[a] Miriam Simón-Fuentes[a] Emmanuel Orta-Zavalza[a] Rafael Samaniego[b] Paloma Sánchez-Mateos[b] María Escribese[c] Francisco J. Cimas[d] Matilde Bustos[e] Mario Pérez-Diego[a] Alberto Ocaña[d] Ángeles Domínguez-Soto[a] Miguel A. Vega[a] Ángel L. Corbí[a]

[a]Centro de Investigaciones Biológicas, CSIC, Madrid, Spain; [b]Instituto de Investigación Sanitaria Gregorio Marañón (IiSGM), Laboratorio de Inmuno-Oncología, Madrid, Spain; [c]Institute for Applied Molecular Medicine, School of Medicine, Universidad CEU San Pablo, Madrid, Spain; [d]Instituto de Investigación Sanitaria (IdISSC) and CIBERONC, Medical Oncology Department, Experimental Therapeutics Unit, Hospital Clínico San Carlos (HCSC), Madrid, Spain; [e]Institute of Biomedicine in Seville (IBiS), Campus del Hospital "Virgen del Rocío", Sevilla, Spain

Keywords
Macrophage · Inflammation · Macrophage polarization · Interleukin-10

Abstract
During inflammatory responses, monocytes are recruited into inflamed tissues, where they become monocyte-derived macrophages and acquire pro-inflammatory and tissue-damaging effects in response to the surrounding environment. In fact, monocyte-derived macrophage subsets are major pathogenic cells in inflammatory pathologies. Strikingly, the transcriptome of pathogenic monocyte-derived macrophage subsets resembles the gene profile of macrophage colony-stimulating factor (M-CSF)-primed monocyte-derived human macrophages (M-MØ). As M-MØ display a characteristic cytokine profile after activation (IL-10^{high} TNF^{low} $IL23^{low}$ $IL6^{low}$), we sought to determine the transcriptional signature of M-MØ upon exposure to pathogenic stimuli. Activation of M-MØ led to the acquisition of a distinctive transcriptional profile characterized by the induction of a group of genes (Gene set 1) highly expressed by pathogenic monocyte-derived macrophages in COVID-19 and whose presence in tumor-associated macrophages (TAM) correlates with the expression of macrophage-specific markers (*CD163*, *SPI1*) and *IL10*. Indeed, Gene set 1 expression was primarily dependent on ERK/p38 and STAT3 activation, and transcriptional analysis and neutralization experiments revealed that IL-10 is not only required for the expression of a subset of genes within Gene set 1 but also significantly contributes to the idiosyncratic gene signature of activated M-MØ. Our results indicate that activation of M-CSF-depen-

V.D.C. and M.S.-F. contributed equally to this work, and their order of authorship is arbitrary.
A.D.-S., M.A.V., and A.L.C. contributed equally to this work.

karger@karger.com
www.karger.com/jin

Correspondence to:
Ángel L. Corbí, acorbi@cib.csic.es

dent monocyte-derived macrophages induces a distinctive gene expression profile, which is partially dependent on IL-10, and identifies a gene set potentially helpful for macrophage-centered therapeutic strategies.

Introduction

Under physiological conditions, tissue-resident macrophages perform homeostatic functions in the dermis, heart, gut, liver, spleen, and serous cavities (reviewed in [1]). However, tissue-resident and monocyte-derived tissue-infiltrating macrophages play distinct functional roles during inflammatory responses [2]. Results from mouse models of inflammation have revealed that native resident macrophages exhibit reparative and anti-inflammatory ability, whereas infiltrating macrophages display a more pathogenic and pro-inflammatory signature [3–6]. Likewise, and in human pathology, recruited monocyte-derived macrophages are primarily engaged in promoting inflammation [7–9]. In fact, monocyte-derived macrophage subsets (FCN1+, SPP1+) have been identified as major pathogenic cells in severe COVID-19 [10, 11], lung fibrosis [4, 12–15], and inflammatory diseases such as rheumatoid arthritis, Crohn's disease, ulcerative colitis, and lupus [16]. Of note, the gene expression profile of these pathogenic macrophage subsets resembles that of macrophage colony-stimulating factor (M-CSF)-primed monocyte-derived human macrophages exposed to IFNγ and/or TNF [16], and shows an enrichment of genes regulated by MAFB and MAF [17], the transcription factors that drive the anti-inflammatory/immunosuppressive polarization of M-CSF-primed monocyte-derived human macrophages [18–20] and tumor-associated macrophages (TAM) [21, 22]. Indeed, and in the case of pulmonary fibrosis, M-CSF signaling is required for the persistence of the pathogenic monocyte-derived macrophages [23].

Although M-CSF and granulocyte macrophage colony-stimulating factor (GM-CSF) promote macrophage differentiation and survival [24], both factors exert opposite instructing effects on macrophages [25, 26] and differentially regulate polarization in TAM [25]. M-CSF is constitutively present in serum, is indispensable for tissue-resident and monocyte-derived macrophage differentiation and survival [24, 27, 28], and primes macrophages (M-MØ) for trophic activity [28] and for the acquisition of an anti-inflammatory and immunosuppressive profile ($IL10^{high}$ TNF^{low} $IL23^{low}$ $IL6^{low}$) upon stimulation with pathogenic agents [25, 29–34]. Conversely, GM-CSF is found mostly at sites of tissue inflammation [24, 28] and primes macrophages (GM-MØ) for robust antigen-presenting and pro-inflammatory ($IL-10^{low}$ TNF^{high} $IL23^{high}$ $IL6^{high}$) activity in response to pathogenic stimuli. Accordingly, M-MØ and GM-MØ exhibit different and unique transcriptional profiles [29, 31, 35–37], which are useful to discriminate macrophage subsets under inflammatory conditions in vivo [38, 39].

Macrophage reprogramming has been already proposed as a therapeutic strategy for chronic inflammatory diseases [40]. However, the identification of subset-specific markers to distinguish newly recruited macrophages from tissue-resident macrophages in inflamed tissues is a requisite for the development of macrophage-directed therapeutic interventions for human pathologies without altering host protection or inflammation resolution. Thus, given the role of M-CSF in the generation of pathogenic monocyte-derived macrophages in inflammatory pathologies, we have now determined the signaling and cytokine requirements for the acquisition of the gene expression profile of M-MØ in response to pathogenic stimuli. In this manner, we have identified a set of genes that are exclusively co-expressed by M-MØ under inflammatory conditions, and whose expression relies on ERK/p38 and STAT3 activation, and is partly dependent on IL-10.

Materials and Methods

Generation of Monocyte-Derived Macrophages and ELISA

GM-CSF-polarized macrophages (hereafter termed GM-MØ) and M-CSF-polarized macrophages (hereafter termed M-MØ) were generated from CD14 + monocytes, as previously described [18]. For macrophage activation, cells were treated with 10 ng/mL *E. coli* 055: B5 lipopolysaccharide (LPS; Sigma-Aldrich, MO, USA), 10 μg/mL N-palmitoyl-S-(2,3-bis [palmitoyloxy]-[2RS]-propyl)-(R)-cysteinyl-(S)-seryl-(S)-lysyl-(S)-lysyl-(S)-lysyl-(S)-lysine (PAM3CSK4; Invivogen), 10 μg/mL disulfide-HMGB1 (HMGB1; HMGBiotech), 100 ng/mL CL264 (Invivogen), or 200 μM palmitate prepared as described [41]. Generation of monocyte-derived M-MØ in the presence of tumor-conditioned medium was done as previously described [42], and the neutralizing monoclonal antihuman IL-10 antibody (R&D Systems) was added at a final concentration of 2.5 μg/mL. For intracellular signaling inhibition, macrophages were exposed to p38MAPK inhibitor BIRB0796 (0.1 μM), MEK inhibitor U0126 (2.5 μM), or JNK inhibitor SP600125 (30 μM) for 60 min before treatment with LPS. Cytokine detection was carried out with ELISA kits for human TNF, IL12p40 (BD Biosciences, San Jose, CA, USA), IL-6 (Sigma-Aldrich), CCL19 (Sigma-Aldrich), IL-10 (Biolegend), and IFNβ (PBL Interferon Source) according to the manufacturers' protocols.

Quantitative Real-Time RT-PCR

RNA was quantified as described [18] using the Universal Human Probe library and custom-made microfluidic gene cards

(Roche Diagnostics, Mannheim, Germany). Gene-specific oligonucleotides were designed using the Universal Probe Library software (Roche Diagnostics). Assays were made in duplicate on 3 independent samples of each type and the results normalized according to the mean of the expression level of endogenous reference genes *HPRT1*, *TBP*, and *RPLP0*. In all cases, the results were expressed using the ΔΔCT method for quantitation.

Western Blot

Western blot was carried out following previously described procedures [18] and using antibodies against phosphorylated and total ERK1/2, p38MAPK, and JNK (Cell Signaling); phosphorylated and total STAT1 and STAT3 (BD Biosciences); IκBα, phosphorylated IRF3, and phosphorylated CREB (Cell Signaling); and SOCS2 (sc-9022, Santa Cruz, CA, USA). Protein loading was normalized using a monoclonal antibody against GAPDH (sc-32233, Santa Cruz, CA, USA), β-actin (Sigma-Aldrich), or α-tubulin (sc-58667, Santa Cruz, CA, USA).

Microarray and RNAseq Analysis

Global gene expression analysis was performed on RNA obtained from 3 independent samples of untreated (M-MØ or GM-MØ) or LPS-treated human monocyte-derived macrophages (4 h, M-MØ + LPS or GM-MØ + LPS). RNA isolation, microarray analysis (whole human genome microarray, Agilent Technologies, Palo Alto, CA, USA), and statistical treatment of microarray data were performed following previously described procedures [18]. Microarray data were deposited in Gene Expression Omnibus (GEO) (http://www.ncbi.nlm.nih.gov/geo/) under accession no. GSE99056. The differentially expressed genes were analyzed for annotated gene set enrichment using the online tool ENRICHR (http://amp.pharm.mssm.edu/Enrichr/) [43]. For gene set enrichment analysis (GSEA) (http://software.broadinstitute.org/gsea/index.jsp) [44], the gene sets available at the website, as well as previously defined gene sets [37], were used. For RNAseq, total RNA was extracted from 3 independent preparations of M-MØ exposed to LPS, CL264, or palmitate (C16:0) for 0.5, 2, 4, or 12 h, and library preparation, fragmentation, and sequencing were performed at BGI (https://www.bgitechsolutions.com) using the BGISEQ-500 platform, and data were deposited in GEO (http://www.ncbi.nlm.nih.gov/geo/) under accession no. GSE156921. An average of 4.48 Gb clean reads were generated per sample and, after filtering, the clean reads were mapped to the reference (UCSC Genome assembly hg38) using Bowtie2 (average mapping ratio 91.82%) [45]. In addition, RNAseq (https://www.bgitechsolutions.com, BGISEQ-500 platform) was done on 3 independent preparations of M-MØ exposed to LPS for 4 h after transfection with either a control siRNA or an STAT3-specific siRNA (Dharmacon), and data were deposited in GEO under accession no. GSE180897. A similar procedure was used to perform RNAseq on 3 independent preparations of M-MØ exposed to LPS for 4 h in the presence of either an anti-IL-10 neutralizing monoclonal antibody (2.5 μg/mL, R&D Systems) or an isotype-matched antibody, and data were deposited in GEO under accession no. GSE181250. Gene expression levels were calculated by using the RSEM software package [46], and differential gene expression was assessed by using the R-package DESeq2 algorithms using the parameters Fold Change >2 and adjusted p value <0.05. Semantic similarities and enrichment analysis among DO terms and cluster 1 gene set were assessed by using the R packages DOSE and clusterProfiler [47, 48]. As universe genes (background genes), all annotated genes derived from the limma microarray analysis comparing M-MØ versus M-MØ + LPS and with signal intensity values above background values were considered.

Immunohistochemistry

Human biopsied samples were obtained from patients undergoing surgical treatment and following the Medical Ethics Committee procedures of Hospital General Universitario Gregorio Marañón. For fluorescence and confocal microscopy, cryosections and imaging were performed as previously described [18]. Quantification of in vivo protein expression, using the mean fluorescence intensities of the proteins of interest (SOCS2, BMP6, CCL19, and PDGFA), was done as reported [18]. The antibodies used were the following: mouse monoclonal anti-CD163 (K0147-4, MBL), rabbit polyclonal anti-PDGFA and rabbit polyclonal anti-SOCS2 (sc-127 and sc-9022; Santa Cruz, CA, USA), goat polyclonal anti-BMP6 (AF507; R&D Systems), and rabbit polyclonal anti-CCL19 (13397-1-AP; Proteintech). Double-immunofluorescence for CD163 and CCL19 was performed on tissue microarrays from archival formalin-fixed paraffin-embedded (FFPE) resection specimens from patients with breast tumor who underwent curative intent surgery (mastectomies and segmental resections) at Hospital Universitario Virgen del Rocio (HUVR, Seville, Spain). All samples were histopathologically verified and selected by a specialized surgical pathologist prior to analysis. Ethical permission for the study was approved by the Ethical Committee at HUVR. After deparaffinization, rehydration, and antigen-retrieval using the automated PT Link system (Dako, Agilent Technologies), tissue microarray slides were incubated with a mixture of a mouse monoclonal antihuman CD163 (NB110-59935; Novus Biologicals) and a rabbit polyclonal antihuman CCL19 (NBP2-56275; Novus Biologicals) overnight at 4°C. Samples were washed 3 times with PBS and then incubated with Alexa-488-conjugated goat anti-mouse IgG and Alexa-568-conjugated donkey-anti-rabbit IgG (Invitrogen). The slices were incubated at 37°C for 45 min, and nuclear staining was performed with DAPI. Coverslips were mounted with fluorescent mounting medium onto glass slides and examined with confocal microcopy (Leica TCS SP2 AOBS; Leica Microsystems).

Statistical Analysis

For comparison of means, and unless otherwise indicated, statistical significance of the generated data was evaluated using the Student's t test. In all cases, $p < 0.05$ was considered as statistically significant.

Results

Differential Activation of ERK and p38 Underlies the Opposite Cytokine Profiles of Activated M-CSF-Primed (M-Mø) and GM-CSF-Primed (GM-Mø) Monocyte-Derived Macrophages

To determine the molecular basis for the acquisition of the cytokine profile of activated M-MØ ($IL10^{high}$ TNF^{low} $IL12^{low}$ $IL6^{low}$) [29–31], we analyzed the kinetics of cytokine production of both M-MØ and GM-MØ mac-

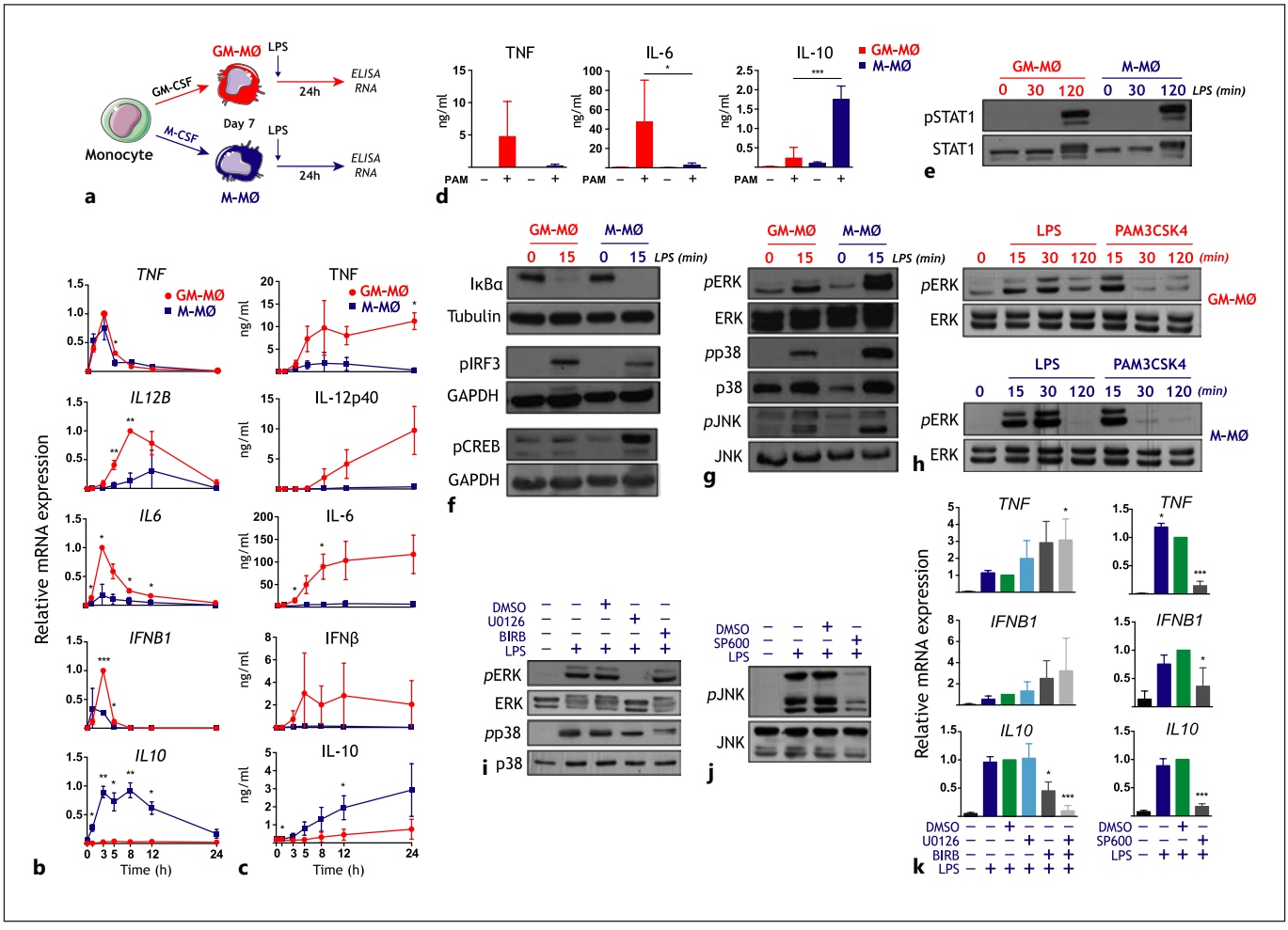

Fig. 1. Cytokine profile and intracellular signaling of activated M-MØ and GM-MØ. **a** Experimental design. **b**, **c** Kinetics of LPS-induced cytokine mRNA (**b**) and protein (**c**) expression of M-MØ and GM-MØ. Results are expressed relative to the maximal level of cytokine mRNA (**b**) and the concentration of the indicated cytokines (**c**) in GM-MØ (TNF, IL-12p40, IL-6, IFNβ) or M-MØ (IL-10). Shown are the means and SD of 3 independent experiments ($n = 3$; *, $p < 0.05$; **, $p < 0.005$). **d** PAM3CSK4 (PAM)-induced cytokine production of M-MØ and GM-MØ. Shown are the means and SD of 6 independent experiments ($n = 6$; *, $p < 0.05$; ***, $p < 0.0005$). **e**, **f** M-MØ and GM-MØ were treated with LPS, and cell lysates were obtained at the indicated time points and assayed for the expression of phosphorylated and total STAT1 (**e**), IκBα, phosphorylated CREB, and phosphorylated IRF3 (**f**) by Western blot using specific antibodies. Protein loading was normalized using a monoclonal antibody against GAPDH or α-tubulin. **g**, **h** M-MØ and GM-MØ were treated with LPS or PAM3CSK4, and cell lysates obtained at the indicated time points were assayed for the expression of phosphorylated and total ERK1/2 (**g**, **h**), p38MAPK (**g**), and JNK (**g**) by Western blot using specific antibodies. **i**, **j** Total and phosphorylated ERK, p38MAPK, and JNK levels in untreated and LPS-treated M-MØ in the absence (−) or presence of the MEK inhibitor U0126 (U0) (**i**), the p38MAPK inhibitor BIRB0796 (BIRB) (**i**), the JNK inhibitor SP600125 (SP600) (**j**), or DMSO as a vehicle control. **k** LPS-induced cytokine mRNA levels in M-MØ in the absence (−) or presence of U0126 (U0), BIRB0796 (BIRB), SP600125 (SP600), or DMSO as a vehicle control. Results are expressed relative to the level of each cytokine mRNA after LPS + DMSO treatment. Shown are the means and SD of 4 independent experiments ($n = 4$; *, $p < 0.05$; **, $p < 0.005$; ***, $p < 0.0005$). LPS, lipopolysaccharide; M-MØ, monocyte-derived human macrophages.

rophage subtypes after exposure to LPS (Fig. 1a). After 3–5 h, LPS induced significantly elevated levels of IL-10 mRNA only in M-MØ, a time at which *IL12B*, *IL6*, and *IFNB1* mRNA were significantly higher in GM-MØ (Fig. 1b), with all these transcriptional changes preceding the characteristic LPS-induced cytokine production of GM-MØ and M-MØ (Fig. 1c). Of note, the IL10^{high} cytokine profile of activated M-MØ was similarly gained upon exposure to the TLR2 ligand PAM3CSK4 (Fig. 1d). Next, we compared the LPS-induced intracellular signaling in

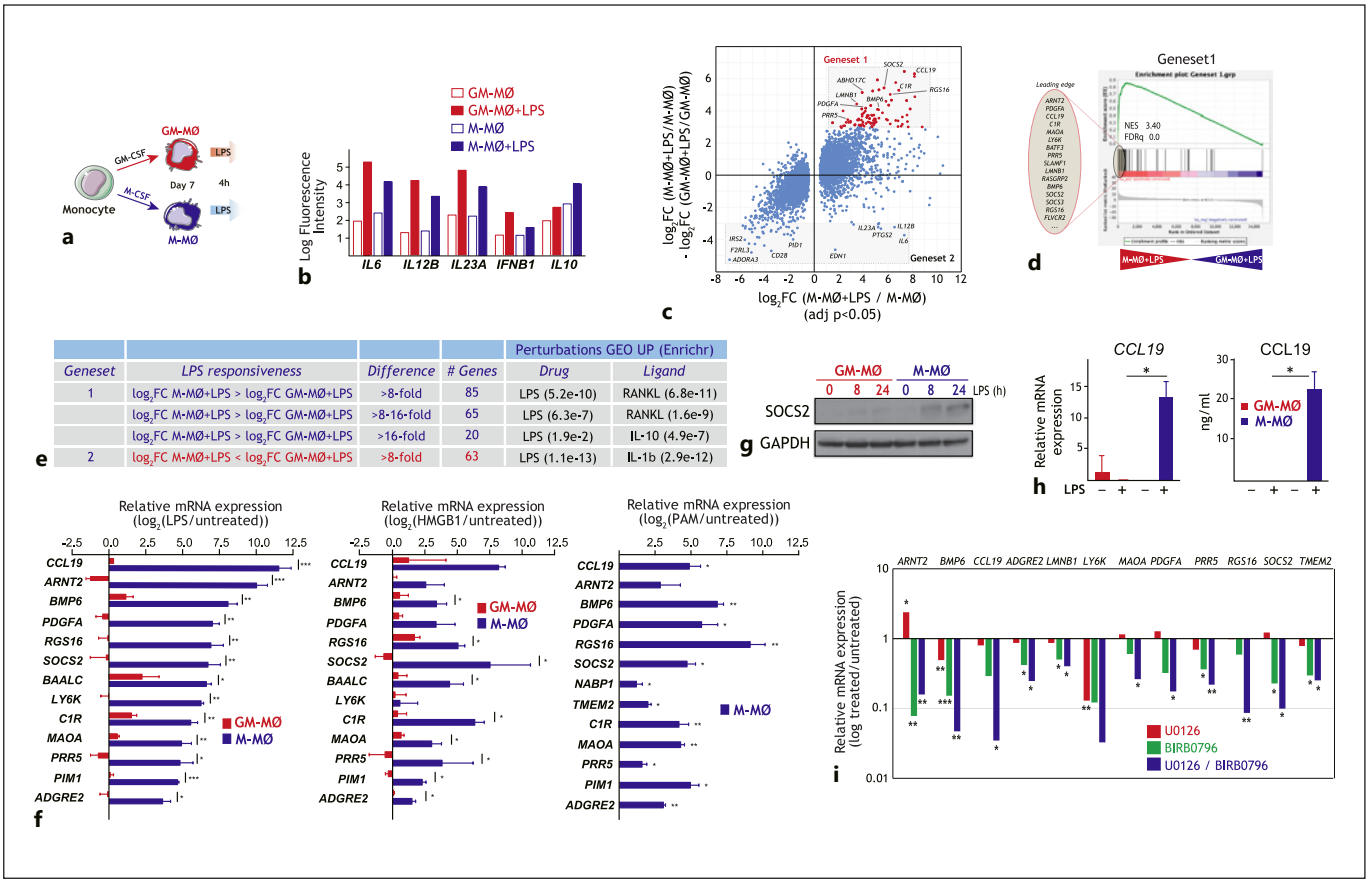

Fig. 2. Identification of genes differentially regulated by LPS in M-MØ and GM-MØ. **a** Experimental design. **b** Normalized fluorescence intensity of the indicated cytokine mRNA in untreated and LPS-treated M-MØ and GM-MØ. **c** Scatter plot of microarray results, showing the LPS-induced gene expression changes in M-MØ (log_2 M-MØ + LPS/M-MØ, adj $p < 0.05$, *x*-axis) plotted against the difference in the LPS-induced gene expression changes in M-MØ and GM-MØ (log_2FC [M-MØ + LPS/M-MØ] – log_2FC [GM-MØ + LPS/GM-MØ]) (*y*-axis). The relative position of some informative genes is indicated. **d** GSEA on the ranked list of genes obtained from the comparison of the transcriptome of M-MØ + LPS versus GM-MØ + LPS using Gene set 1 genes. The identity of the genes within the leading edge is shown. **e** Identification of the gene sets including genes with the highest differential LPS responsiveness in M-MØ (Gene set 1) and GM-MØ (Gene set 2). The number of genes in each gene set and associated gene ontology terms (Enrichr) are indicated. **f** Expression of selected members of Gene set 1 in untreated and LPS-treated M-MØ and GM-MØ (left panel), untreated and HMGB1-treated M-MØ and GM-MØ (middle panel), and untreated and PAM3CSK4-treated M-MØ (right panel), as determined by qRT-PCR on 4 independent samples. Results are indicated as the mRNA levels of each gene in activated cells relative to the level of the same mRNA in untreated cells (n = 3–4; *, $p < 0.05$; **, $p < 0.005$; ***, $p < 0.0005$). **g** SOCS2 protein levels in GM-MØ and M-MØ stimulated with LPS for the indicated times, as determined by Western blot. Shown is 1 representative experiment ($n = 2$). **h***CCL19* mRNA and CCL19 protein levels in untreated (–) and LPS-treated M-MØ and GM-MØ. Shown are the means and SD of 5 independent experiments ($n = 5$; *, $p < 0.05$). **i** Expression of the indicated Gene set 1 genes in M-MØ stimulated with LPS (4 h) in the presence of U0126, BIRB0796, or BIRB0796 and U0126. Results indicate the expression of each gene relative to its expression in LPS-stimulated M-MØ. Shown are the means and SD of 3–4 independent experiments (n = 3–4; *, $p <$ 0.05; **, $p < 0.01$; ***, $p < 0.005$). LPS, lipopolysaccharide; GSEA, gene set enrichment analysis; M-MØ, monocyte-derived human macrophages.

M-MØ and GM-MØ. LPS triggered similar levels of NFκB and STAT1 activation in both GM-MØ and M-MØ (Fig. 1e, f, online suppl. Fig. 1a; for all online suppl. material, see www.karger.com/doi/10.1159/000519305), whereas LPS induced CREB phosphorylation exclusively in M-MØ (Fig. 1f, online suppl. Fig. 1a), and LPS-induced phosphorylation of IRF3 [49] was higher in GM-MØ (Fig. 1f, online suppl. Fig. 1a), in accordance with their higher production of IFNβ. In addition, phosphorylation of ERK, JNK, and p38 was higher in LPS- or PAM3CSK4-treated

M-MØ than in activated GM-MØ (Fig. 1g, h, online suppl. Fig. 1b). Since IL-10 is preferentially produced by LPS-treated M-MØ (Fig. 1b, c), and given that ERK and p38 activation contribute to LPS-induced IL-10 expression [50, 51], we tested whether pretreatment of M-MØ with inhibitors of MEK-ERK (U0126), JNK (SP600125), or p38MAPK (BIRB0796) (Fig. 1i, j) affected the production of cytokines from LPS-treated M-MØ. Importantly, the simultaneous inhibition of ERK and p38 activation significantly impaired the LPS-induced *IL10* mRNA expression but enhanced LPS-induced *TNF* mRNA levels (Fig. 1k). Therefore, LPS-induced activation of ERK and p38 underlies the paradigmatic cytokine profile of M-MØ.

Identification of a Set of Genes Specifically Modulated upon M-Mø Activation

To find out whether the distinct LPS-induced intracellular signaling in LPS-activated GM-MØ and M-MØ results in wider transcriptional differences, we next determined their respective gene signatures after a 4-h exposure to LPS (Fig. 2a). Transcriptional data (deposited in GEO, GSE99056) confirmed the distinct cytokine mRNA profile of LPS-treated M-MØ and GM-MØ (Fig. 2b), and revealed extensive differences in their respective LPS-triggered gene signatures, thus allowing the identification of genes whose LPS responsiveness greatly differed between M-MØ and GM-MØ (Fig. 2c). Specifically, and using an 8-fold difference between the LPS-induced upregulation in M-MØ and GM-MØ as a threshold, 85 genes were found to be preferentially upregulated by LPS in M-MØ (termed Gene set 1) (Fig. 2d), while 63 genes were preferentially upregulated by LPS in GM-MØ (termed Gene set 2) (Fig. 2c; online suppl. Table 1). Although both gene sets were enriched in LPS-responsive genes, Gene set 1 was significantly enriched in IL-10-responsive genes, in line with the anti-inflammatory and immunosuppressive functions of M-MØ (Fig. 2e). Conversely, Gene set 2 was enriched in IL-1β-regulated genes (Fig. 2e), in agreement with the pro-inflammatory capabilities of GM-MØ. Analysis of independent validation samples confirmed the restricted upregulation of the genes with the strongest M-MØ-specific LPS-inducibility of Gene set 1 (Fig. 2f) that, in fact, were also preferentially upregulated in M-MØ upon activation with the alarmin HMGB1 [52], and also upregulated after exposure to the TLR2 ligand PAM3CSK4 (Fig. 2f). Further confirming their activation-induced expression, GSEA and clustering analysis showed that global Gene set 1 expression was significantly upregulated in M-MØ upon activation by LPS, the TLR7 ligand CL264, or palmitate (online suppl. Fig. 2a–c), 3 stimuli which differ in their IL-10-inducing capacity (online suppl. Fig. 2d) [41, 53].

Besides, and in line with the transcriptional data, the M-MØ-specific LPS-inducibility of Gene set 1 was verified at the protein level. As representative examples, SOCS2 protein was exclusively detected in LPS-treated M-MØ, which also secreted detectable levels of CCL19 (Fig. 2g, h). Therefore, M-MØ activation results in the acquisition of a transcriptome that differs from that of GM-MØ and that is best characterized by the expression of the Gene set 1 group of genes. Interestingly, and like the case of IL-10 (Fig. 1k), upregulation of the genes with the strongest M-MØ-specific LPS-inducibility of Gene set 1 was impaired in the presence of inhibitors of ERK and p38 activation (Fig. 2i). Therefore, the M-MØ-specific LPS-mediated upregulation of Gene set 1 expression is primarily dependent on the activation of ERK and p38.

Pathological Correlates of Gene Set 1 Expression in vivo

To address the potential significance of Gene set 1 expression in settings where monocyte-derived macrophages contribute to pathology, Gene set 1 expression in COVID-19 and hyperproliferative diseases was analyzed . In the case of COVID-19, the gene profile of M-MØ + LPS showed a significant overrepresentation of genes overexpressed in macrophages from severe COVID-19 patients' bronchoalveolar lavage (BALF) [54–56] (Fig. 3a). Moreover, M-MØ + LPS exhibited an overrepresentation of the genes that characterize the COVID-19 pathogenic monocyte-derived alveolar macrophage subsets that have been identified in 3 independent studies (groups 1–3, MoAM1-3, CXCL10+/CCL2+) [10, 11, 16] (Fig. 3b). Conversely, the transcriptome of GM-MØ + LPS appeared enriched in genes that characterize subsets of resident alveolar macrophages in the same reports [10, 11, 16] (Fig. 3b). In agreement with these correlations, Gene set 1 was significantly enriched in various "COVID-19-related gene sets" (Enrichr, Fig. 3c) as well as in the transcriptome of peripheral blood mononuclear cells from COVID-19 patients [57] (Fig. 3d). Regarding hyperproliferative diseases, analysis of proteins encoded by Gene set 1 genes with a strong M-MØ-specific LPS-inducibility (e.g., *CCL19*, *BMP6*, *SOCS2*, *PDGFA*) revealed the expression of CCL19 in breast cancer $CD163^+$ TAM, which are M-CSF-dependent [58] (online suppl. Fig. 3a); the co-expression of SOCS2 and BMP6 in $CD163^+$ melanoma TAM (online suppl. Fig. 3b); and the co-expression of CCL19, PDGFA, BMP6, and SOCS2 proteins in $CD163^+$ nevus-associated macrophages (online suppl.

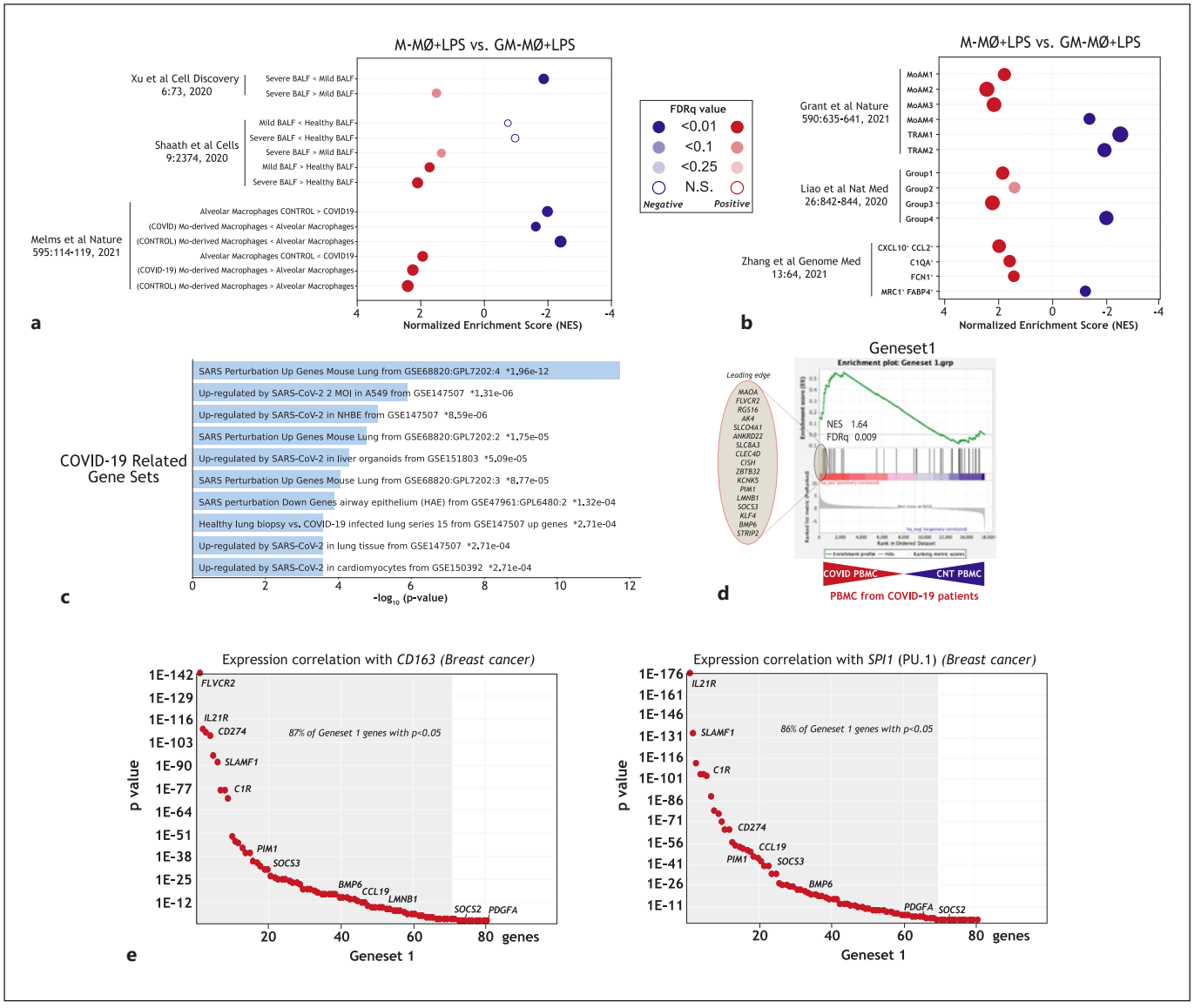

Fig. 3. *In vivo* co-expression of Gene set 1. **a**, **b** Summary of GSEA on the ranked list of genes from the comparison of the transcriptome of M-MØ + LPS and GM-MØ + LPS using previously defined gene sets for (**a**) COVID-19 BALF macrophages [54–56] or (**b**) COVID-19 pathogenic monocyte-derived macrophage subsets [10, 11, 16]. **c** Gene ontology of Gene set 1 on the "COVID-19-related gene sets" database using Enrichr. **d** GSEA on the ranked list of the comparison of the transcriptome of PBMC from COVID-19 patients versus control PBMC [57], using Gene set 1 genes. The identity of the genes within the leading edge is shown. **e** Correlation of the expression on Gene set 1 genes with the expression of *CD163* or *SPI1* in breast carcinoma, as calculated using TIMER (http://timer.cistrome.org), with indication of the percentage of Gene set 1 genes whose positive correlation with the indicated gene is $p < 0.05$. LPS, lipopolysaccharide; GSEA, gene set enrichment analysis; BALF, bronchoalveolar lavage; PBMC, peripheral blood mononuclear cells; M-MØ, monocyte-derived human macrophages.

Fig. 3c), where a high correlation among the expression of the 4 proteins was found (online suppl. Fig. 3d). Furthermore, Gene set 1 expression was overrepresented in several neoplasms (DisGenet database, online suppl. Fig. 3e) as well as in synovial macrophages from RA patients [59] (online suppl. Fig. 3f) and alveolar macrophages after in vivo LPS instillation in humans [60] (online suppl. Fig. 3g). In fact, Tumor Immune Estimation Resource (TIMER; https://cistrome.shinyapps.io/timer/) [61] analysis revealed a very good correlation between the expression of characteristic macrophage-specific genes (*CD163*, *SPI1*) and the expression of most Gene set 1

genes (86–87%) in breast invasive carcinoma (TCGA cohort, Fig. 3e), where M-CSF and M-CSF-conditioned macrophages have a well-established pathological role [58, 62, 63]. Taken together, all these evidences support the in vivo co-expression of Gene set 1 genes in macrophages within inflammatory and hyperproliferative settings.

STAT-3 and IL-10 Mediates the LPS-Induced Acquisition of a Subset of Gene Set 1: Pathological Significance

Since ERK and p38 activation mediates the LPS-induction of IL-10 [50, 51] (Fig. 1k) and Gene set 1 expression (Fig. 2i), we next conjectured that IL-10 itself might contribute to the expression of Gene set 1. In support of this

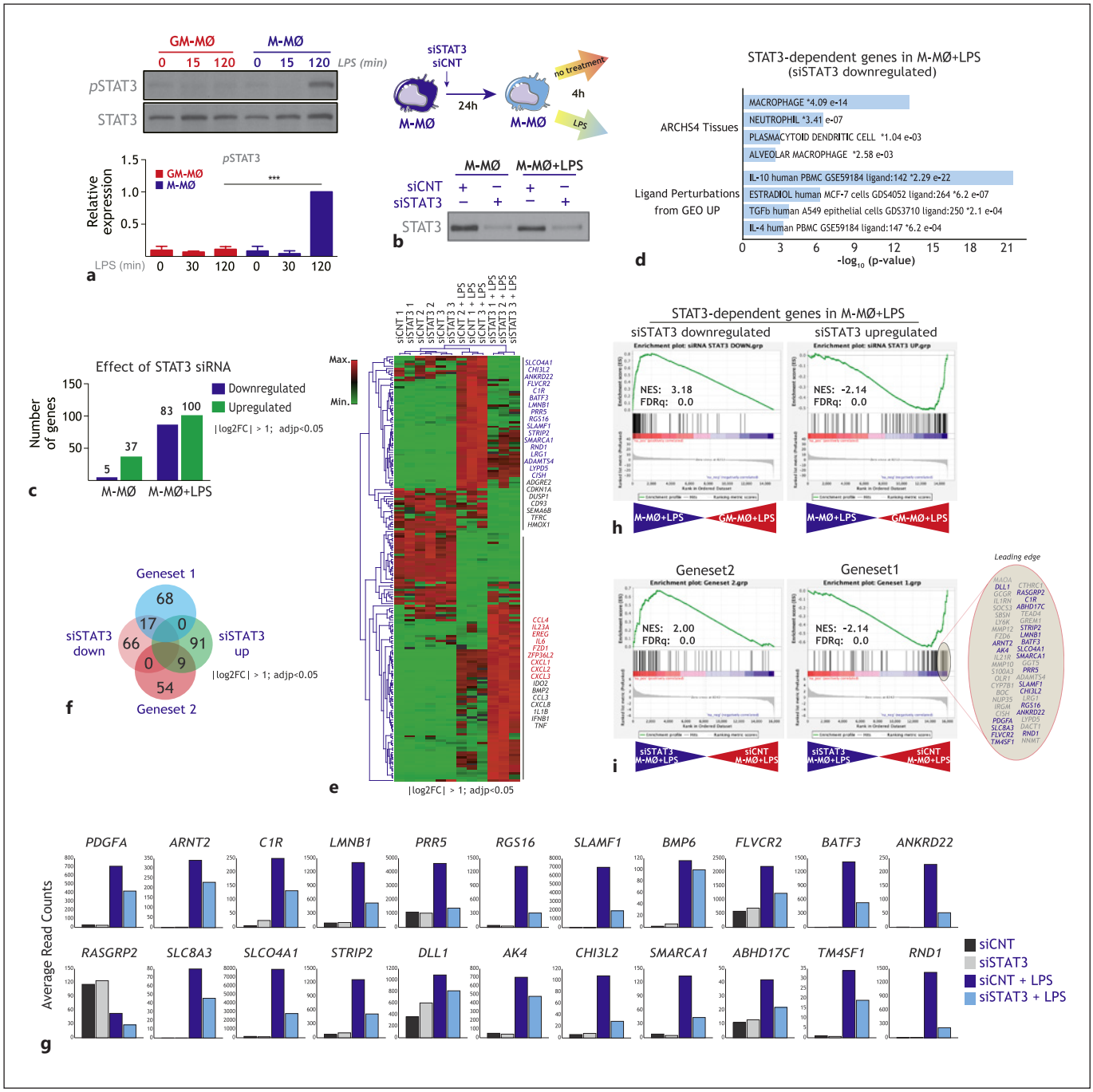

4

(For legend see next page.)

hypothesis, phosphorylation of STAT3, a critical effector of IL-10 [51], was detected at late time points after LPS stimulation in M-MØ but not in GM-MØ (Fig. 4a). Thus, we first assessed the involvement of STAT3 in the LPS-inducibility of Gene set 1 genes by knocking down the expression of STAT3 before LPS stimulation (Fig. 4b). Determination of the STAT3-dependent transcriptome of both M-MØ and M-MØ+LPS evidenced that STAT3 has a significant effect on the gene expression profile of LPS-treated M-MØ, as STAT3 knockdown significantly (log-2FC <1; adjp <0.05) altered the expression of 183 genes (83 downregulated; 100 upregulated) (Fig. 4c). Of note, STAT3 knockdown significantly impaired the expression of 20% of the genes within M-MØ + LPS-specific Gene set 1 (17 out of 85) and, concomitantly, enhanced the expression of 15% of the GM-MØ + LPS-specific Gene set 2 (Fig. 4e–g). Indeed, GSEA revealed that the transcriptome of LPS-treated M-MØ was greatly enriched in genes whose expression is dependent on STAT3 (Fig. 4h) and that knockdown of STAT3 results in a very significant downregulation of genes within Gene set 1 (Fig. 4i). Conversely, the transcriptome of LPS-treated GM-MØ showed an over-representation of genes whose expression increases upon STAT3 knockdown (Fig. 4h) and that knockdown of STAT3 leads to a significant upregulation of Gene set 2 genes (Fig. 4i). Taken together, this set of experiments illustrates that the activation of STAT3 notably contributes to the acquisition of the LPS-treated M-MØ transcriptome and, more specifically, to the expression of Gene set 1.

Since STAT3 is a major effector of IL-10 [51], we next tested the involvement of IL-10 in Gene set 1 expression. To that end, M-MØ were exposed to LPS (4 h) in the presence of an anti-IL-10 neutralizing monoclonal antibody, and the resulting transcriptomes were compared (Fig. 5a). Blockade of IL-10 significantly (adjp <0.05) reduced the LPS-inducibility of 254 genes and potentiated the LPS-mediated upregulation of 248 genes (Fig. 5a), with most of the 254 IL-10-upregulated genes being strongly increased by LPS in M-MØ (Fig. 5b). Noteworthy, the LPS-upregulated expression of one-third (22) of the genes in Gene set 1 was significantly inhibited in the presence of a blocking antibody against anti-IL-10 (Fig. 5c, d), implying that the expression of a significant number of genes within Gene set 1 is IL-10-dependent. Furthermore, a good overlap was seen between IL-10-dependent and STAT3-dependent Gene set 1 genes, as the expression of 76% of genes affected by STAT3 knockdown was also impaired by the presence of the neutralizing anti-IL-10 antibody (13 out of 17, Fig. 5c). However, analysis of the IL-10-dependency of Gene set 1 also evidenced the existence of genes within Gene set 1 whose expression is IL-10-independent (Fig. 5e). The IL-10-dependency of the genes identified in Fig. 5c–e was further validated through the use of the anti-IL-10 blocking antibody on an independent set of M-MØ validation samples (Fig. 5f). Noteworthy, these confirmatory set of experiments not only substantiated the presence of IL-10-dependent and independent genes in Gene set 1 but also revealed the relevant

Fig. 4. Contribution of STAT3 to the acquisition of Gene set 1 expression. (**a**) M-MØ and GM-MØ were treated with LPS, and cell lysates obtained at the indicated time points and assayed for the expression of phosphorylated and total STAT3 by Western blot using specific antibodies. (Lower panel) Densitometric analysis of the experiment shown above. **b** Experimental design for the RNA-seq analysis on M-MØ transfected with a control (siCNT) or a STAT3-specific siRNA (siSTAT3) before exposure to LPS for 4 h (GSE180897) (lower panel) STAT3 protein expression in M-MØ transfected with control siRNA (siCNT) or a STAT3-specific siRNA (siSTAT3), and either before (untreated) or after LPS stimulation ($n = 3$). **c** Number of genes whose expression is significantly ($\log_2$FC > [1]; adjusted $p < 0.05$) enhanced or reduced in either M-MØ or M-MØ exposed to LPS. **d** Gene ontology of the 83 STAT3-dependent genes in M-MØ + LPS on the "ARCHS4 Tissues" and "Ligand Perturbations from GEO UP" databases using Enrichr. **e** Heatmap of the expression of genes significantly (log-2FC >1; adjp <0.05) modulated by STAT3-specific siRNA in 3 independent samples of untreated or LPS-treated M-MØ, as determined by RNAseq and using Genesis (https://genome.tugraz.at/genesisclient/genesisclient_description.shtml). Selected genes for each cluster are indicated, highlighting those within Gene set 1 (blue) or Gene set 2 (red). **f** Venn diagram comparing the genes in Gene set 1 or Gene set 2 with the genes whose expression in M-MØ + LPS is significantly (log2FC >1; adjp <0.05) modulated by STAT3-specific siRNA. **g** Expression of the indicated Gene set 1 genes in M-MØ transfected with control siRNA (siCNT) or a STAT3-specific siRNA (siSTAT3) either before or after stimulation with LPS (4 h) (GSE180897). **h** GSEA (http://software.broadinstitute.org/gsea/index.jsp) of the ranked comparison of the transcriptomes of M-MØ + LPS versus M-MØ + LPS, using the genes whose expression in M-MØ + LPS is significantly (log2FC >1; adjp <0.05) modulated (upregulated or downregulated) by STAT3-specific siRNA. NES and FDRq are indicated in each case. The identity of the genes within the leading edge is shown. **i** GSEA (http://software.broadinstitute.org/gsea/index.jsp) of the ranked comparison of the transcriptomes of siSTAT3-M-MØ + LPS versus siCNT-M-MØ + LPS, using Gene set 1 or Gene set 2. NES and FDRq are indicated in each case. The identity of the genes within the leading edge is shown for Gene set 1, with indication of IL-10-dependent genes indicated in Fig. 5 (blue). LPS, lipopolysaccharide; FDRq, false discovery rate q value; NES, normalized enrichment score; GSEA, gene set enrichment analysis; M-MØ, monocyte-derived human macrophages.

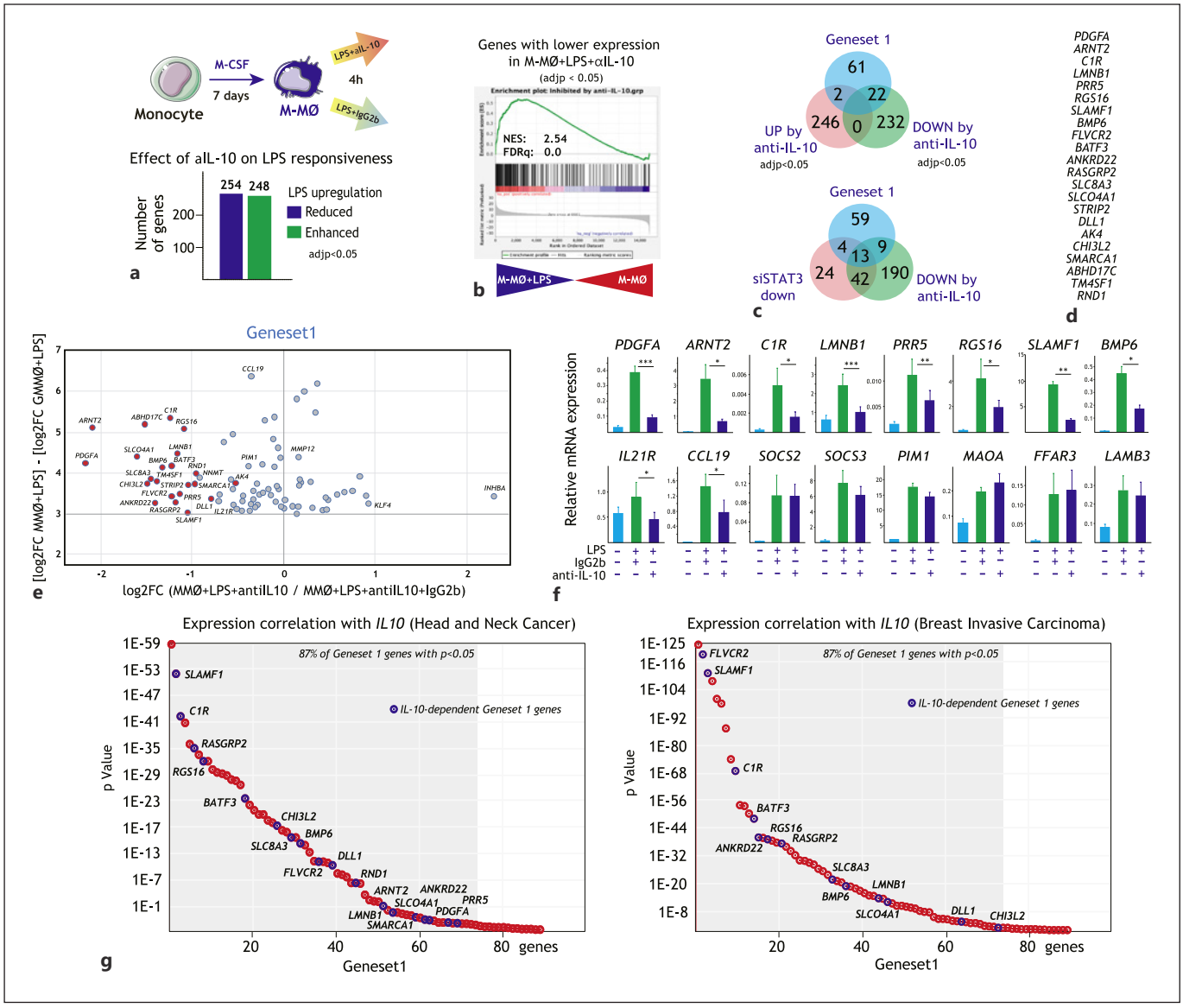

Fig. 5. Contribution of IL-10 to the acquisition of Gene set 1 expression. **a** Experimental design for the RNAseq analysis on M-MØ exposed to LPS in the presence of a blocking anti-IL-10 antibody (anti-IL-10) or an isotype-matched antibody (IgG) (GSE181250). (Lower panel) Number of genes whose LPS-regulated expression is significantly (log_2FC> [1]; adjusted $p < 0.05$) enhanced or reduced in M-MØ exposed to LPS in the presence of a blocking anti-IL-10 antibody (anti-IL-10). **b** GSEA (http://software.broadinstitute.org/gsea/index.jsp) of the statistics-ranked list of genes obtained from the M-MØ + LPS versus untreated M-MØ limma analysis, using the genes whose LPS-inducibility is significantly reduced by anti-IL-10 as data set. Normalized Enrichment Score (NES) and FDRq are indicated in each case. **c** (Upper panel) Venn diagram comparing the genes in Gene set 1 with the genes whose LPS regulation is significantly affected by a blocking anti-IL-10 antibody. (Lower panel) Venn diagram comparing the genes in Gene set 1 with the genes whose LPS regulation is downregulated by either STAT3 knockdown or a blocking anti-IL-10 antibody. **d** List of IL-10-dependent genes in Gene set 1. **e** Scatter plot on the genes with the highest M-MØ-specific LPS-upregulation, showing their LPS-induced gene expression change (log_2FC MMO + LPS – log_2FC GMMO + LPS, *y*-axis) plotted against their respective susceptibility to the presence of a blocking anti-IL-10 antibody (log_2FC (anti-IL10/IgG2b), *x*-axis). The position of some informative genes is indicated. **f** Expression of the indicated Gene set 1 genes in LPS-stimulated M-MØ in the presence of a blocking anti-IL-10 antibody (anti-IL-10) or an isotype-matched antibody (IgG). Results indicate the expression of each gene relative to its expression in non-stimulated M-MØ. Shown are the means and SD of 3 independent experiments ($n = 6$; *, $p < 0.05$; ***, $p < 0.005$). **g** Correlation of the expression on Gene set 1 genes with the expression of *IL10* in breast carcinoma (right panel) and head and neck cancer (left panel), as calculated using TIMER (http://timer.cistrome.org), with indication of the percentage of Gene set 1 genes whose positive correlation with the indicated gene is $p < 0.05$. LPS, lipopolysaccharide; FDRq, false discovery rate *q* value; GSEA, gene set enrichment analysis; M-MØ, monocyte-derived human macrophages.

contribution of IL-10 to the expression of genes like *IL21R* and *CCL19* (Fig. 5f), whose IL-10-dependency could be seen when less stringent filtering (paired analysis) was applied on the RNAseq data described in Figure 5a–e. Of note, and lending further relevance to this finding, expression of most genes within Gene set 1 (both IL-10-dependent and independent) very significantly correlated with *IL10* expression in breast invasive carcinoma, where M-CSF-conditioned macrophages are pathological [58, 62, 63], as well as in head and neck cancer (Fig. 5g). Therefore, IL-10 and STAT3 significantly contribute to the expression of genes included within M-MØ + LPS-specific Gene set 1, whose co-expression correlates with that of IL-10 in vivo.

Discussion

Macrophages in inflamed tissues display a wide array of polarization states, whose acquisition is driven by the integration of extracellular cues and depends on macrophage ontogeny [64, 65]. In this regard, tissue-resident and blood-borne tissue-infiltrating macrophages appear to play distinct functional roles during inflammatory responses [2], with tissue-resident macrophages exhibiting reparative and anti-inflammatory capabilities. Transcriptional analysis of macrophage activation states in mice and humans [26, 29, 66, 67] has mainly focused on macrophages primed toward the pro-inflammatory side and mostly after long-term exposure to activating stimuli. However, since the transcriptome of pathogenic monocyte-derived macrophages in various inflammatory pathologies (COVID-19, rheumatoid arthritis, and fibrosis) [4, 10–16] is under the control of factors that mediate the generation of M-CSF-primed macrophages (M-MØ) [17–20], we undertook the determination of the transcriptome of M-MØ after short-term exposure to activating agents. In this manner, we have identified a novel gene set (Gene set 1) whose acquisition is partly dependent on IL-10 and correlates with the expression of macrophage-specific genes in inflammatory settings in vivo.

Single-cell sequencing of BALF immune cells from patients with COVID-19 has allowed the identification of monocyte-derived macrophages as the pathologic macrophage subsets that drive inflammation in severe COVID-19 and other chronic inflammatory diseases (groups 1–3, MoAM1-3, CXCL10+/CCL2+) [10, 11, 16]. The present study reveals that the genes that identify these pathologic monocyte-derived macrophage subsets are highly overrepresented in the transcriptome of LPS-treated M-MØ. Conversely, the transcriptome of GM-MØ + LPS is enriched in genes that characterize subsets of resident alveolar macrophages (group 4, TRAM1-2, MRC1+ FABP4+) [10, 11, 16]. Actually, the significance of the "M-MØ + LPS/GM-MØ + LPS" dichotomy was also evident when comparing the gene profiles of BALF cells from COVID-19 patients with different degrees of severity [54–56], as the transcriptome of M-MØ + LPS showed an overrepresentation of genes associated to the severe pathology. In addition, these results agree with the fact that the gene profiles of pathologic monocyte-derived macrophage subsets in severe COVID-19 are significantly enriched in MAFB- and MAF-regulated genes [17], as these 2 factors shape the transcriptome of M-CSF-primed monocyte-derived human macrophages [18–20].

Among the genes within Gene set 1, the presence of CCL19 and SOCS2 is worth noting as they might significantly determine the effector functions of activated M-CSF-dependent monocyte-derived macrophages. The higher level of SOCS2 in LPS-activated M-MØ is particularly relevant because SOCS2 acts as an anti-inflammatory factor that promotes TRAF6 degradation [68], inhibits TLR4 signaling in macrophages [69], and mediates the anti-inflammatory actions of lipoxins [70, 71] and type I IFN [72], and its levels are diminished in certain inflammatory pathologies [73]. Therefore, the higher levels of SOCS2 could favor the acquisition of a state of refractoriness to TLR stimulation in LPS-activated M-MØ. Regarding CCL19, its elevated production by activated M-MØ is reminiscent of the parallel expression of both CCL19 and IL-10 in the anti-inflammatory response of myeloid cell lines to certain gut-derived bacterial strains [74] and has implications for the role of tissue-resident macrophages during antitumor responses. CCL19 encodes a ligand for CCR7 [75], which determines T-lymphocyte recirculation and dendritic cell migration into lymph nodes [76]. Unlike the alternative CCR7 ligand (CCL21), CCL19 binding to CCR7 leads to receptor desensitization [77, 78]. Therefore, CCL19 produced by activated M-CSF-primed macrophages might impair emigration of dendritic cells and T lymphocytes from tissues toward the lymph nodes, thus inhibiting the generation of immune responses, an activity that would be compatible with the immunoregulatory (IL-10-producing) ability of activated M-CSF-dependent macrophages.

With respect to the mechanism underlying the acquisition of Gene set 1, our results indicate that IL-10 derived from activated M-MØ significantly contributes to the expression of 25% of the genes (22 out of 85) in Gene set 1, a contribution that is higher if a lower statistical

significance threshold is applied. IL-10 is a pleiotropic cytokine with potent immunosuppressive ability on the innate and adaptive immune systems, and strong anti-inflammatory effects [79]. However, IL-10 exerts contradictory actions on tumor immunity because it not only contributes to an immunosuppressive tumor microenvironment but also inhibits the growth of numerous tumors and induces CD8+ T-cell infiltration and cytotoxicity within preestablished tumors [80, 81]. The ability of IL-10 to exert tumor-promoting or tumor-suppressive effects appears to depend on the timing of its secretion and the cellular target [82]. Thus, although the role of the IL-10-dependent Gene set 1 genes in tumor progression is hard to predict, it is tempting to speculate that they globally contribute to tumor progression because their expression also correlates with the expression of the M-CSF-encoding gene *CSF1*, which also potently promotes progression of several tumor types [58, 83] (data not shown). Indeed, and apart from *IL1RN*, *CISH*, *SOCS2*, and *SOCS3*, Gene set 1 includes genes like *CD274*, which codes for the PDL1 ligand of the immune checkpoint PD1 to trigger co-inhibitory signals, and *SLAMF1*, which regulates T-cell co-stimulation and cytokine production [84].

In summary, our results demonstrate the existence of a set of genes (Gene set 1) whose expression is exclusive for activated M-CSF-primed monocyte-derived macrophages and that can be detected in vivo in various inflammatory conditions. The identification of Gene set 1 provides a useful set of tools to assess the prevailing state of macrophage polarization in diseases where deregulated macrophage polarization is pathologically relevant. Further, as macrophage reprogramming has been proposed as a therapeutic strategy for chronic inflammatory diseases [40], the availability of Gene set 1 might facilitate the design or evaluation of therapeutic protocols based on macrophage reprogramming.

Acknowledgement

The authors gratefully acknowledge Dr. Ana Cuenda for the generous gift of MAPK signaling inhibitors.

Statement of Ethics

Research was conducted ethically in accordance with the World Medical Association Declaration of Helsinki. Human biopsied samples were obtained from patients undergoing surgical treatment and following the Medical Ethics Committee procedures of Hospital General Universitario Gregorio Marañón (HGUGM) and Hospital "Virgen del Rocío" (HUVR). Ethical permission was approved by the Ethical Committee at HGUGM (Report number 13/2018) or at HUVR (Protocol number 0800-N-17). In all cases, informed written consent was obtained from each human subject.

Conflict of Interest Statement

The authors have no conflicts of interest to declare.

Funding Sources

This work was supported by grants from Ministerio de Economía y Competitividad (SAF2017-83785-R) to M.A.V. and A.L.C., "Ayudas FUNDACIÓN BBVA a equipos de investigación científica SARS-CoV-2 y COVID-19" to M.A.V. and A.L.C., Grant 201619.31 from Fundació La Marató/TV3 to A.L.C., and Red de Investigación en Enfermedades Reumáticas (RIER, RD16/0012/0007), and cofinanced by the European Regional Development Fund "A way to achieve Europe" (ERDF), to A.L.C. V.D.C. was funded by a Formación de Personal Investigador predoctoral fellowship from MINECO (Grant BES-2012-053864).

Author Contributions

V.D.C., M.E., P.S.M., M.A.V., A.O., A.D.S., and A.L.C. designed the research. V.D.C., M.S.F., R.S., E.O.Z., F.J.C., M.B., M.P.D., and M.A.V. performed experiments and analyzed data. V.D.C., M.A.V., and A.L.C. wrote the manuscript.

Data Availability Statement

All data generated or analyzed during this study are included in this article and its online suppl. material files. Further enquiries can be directed to the corresponding author. Microarray and RNAseq data manuscript that support the findings of this study are openly available in Gene Expression Omnibus (http://www.ncbi.nlm.nih.gov/geo/) under accession nos GSE99056, GSE156921, GSE180897, and GSE181250.

References

1 Hoeffel G, Ginhoux F. Fetal monocytes and the origins of tissue-resident macrophages. Cell Immunol. 2018;330:5–15.
2 Liao X, Shen Y, Zhang R, Sugi K, Vasudevan NT, Alaiti MA, et al. Distinct roles of resident and nonresident macrophages in nonischemic cardiomyopathy. Proc Natl Acad Sci USA. 2018;115(20):E4661–9.
3 Puranik AS, Leaf IA, Jensen MA, Hedayat AF, Saad A, Kim KW, et al. Kidney-resident macrophages promote a proangiogenic environment in the normal and chronically ischemic mouse kidney. Sci Rep. 2018;8(1):13948.

4 Misharin AV, Morales-Nebreda L, Reyfman PA, Cuda CM, Walter JM, McQuattie-Pimentel AC, et al. Monocyte-derived alveolar macrophages drive lung fibrosis and persist in the lung over the life span. J Exp Med. 2017;214(8):2387–404.
5 Zaslona Z, Przybranowski S, Wilke C, van Rooijen N, Teitz-Tennenbaum S, Osterholzer JJ, et al. Resident alveolar macrophages suppress, whereas recruited monocytes promote, allergic lung inflammation in murine models of asthma. J Immunol. 2014;193(8):4245–53.
6 Lavine KJ, Epelman S, Uchida K, Weber KJ, Nichols CG, Schilling JD, et al. Distinct macrophage lineages contribute to disparate patterns of cardiac recovery and remodeling in the neonatal and adult heart. Proc Natl Acad Sci USA. 2014;111(45):16029–34.
7 Udalova IA, Mantovani A, Feldmann M. Macrophage heterogeneity in the context of rheumatoid arthritis. Nat Rev Rheumatol. 2016;12(8):472–85.
8 Italiani P, Boraschi D. Development and functional differentiation of tissue-resident versus monocyte-derived macrophages in inflammatory reactions. Results Probl Cell Differ. 2017;62:23–43.
9 Epelman S, Lavine KJ, Randolph GJ. Origin and functions of tissue macrophages. Immunity. 2014;41(1):21–35.
10 Grant RA, Morales-Nebreda L, Markov NS, Swaminathan S, Querrey M, Guzman ER, et al. Circuits between infected macrophages and T cells in SARS-CoV-2 pneumonia. Nature. 2021;590(7847):635–41.
11 Liao M, Liu Y, Yuan J, Wen Y, Xu G, Zhao J, et al. Single-cell landscape of bronchoalveolar immune cells in patients with COVID-19. Nat Med. 2020;26(6):842–4.
12 Mari B, Crestani B. Dysregulated balance of lung macrophage populations in idiopathic pulmonary fibrosis revealed by single-cell RNA seq: An unstable "ménage-à-trois". Eur Respir J. 2019;54(2).
13 Morse C, Tabib T, Sembrat J, Buschur KL, Bittar HT, Valenzi E, et al. Proliferating SPP1/MERTK-expressing macrophages in idiopathic pulmonary fibrosis. Eur Respir J. 2019;54(2):1802441.
14 Aran D, Looney AP, Liu L, Wu E, Fong V, Hsu A, et al. Reference-based analysis of lung single-cell sequencing reveals a transitional profibrotic macrophage. Nat Immunol. 2019;20(2):163–72.
15 Reyfman PA, Walter JM, Joshi N, Anekalla KR, McQuattie-Pimentel AC, Chiu S, et al. Single-cell transcriptomic analysis of human lung provides insights into the pathobiology of pulmonary fibrosis. Am J Respir Crit Care Med. 2019;199(12):1517–36.
16 Zhang F, Mears JR, Shakib L, Beynor JI, Shanaj S, Korsunsky I, et al. IFN-γ and TNF-α drive a CXCL10+ CCL2+ macrophage phenotype expanded in severe COVID-19 lungs and inflammatory diseases with tissue inflammation. Genome Med. 2021;13(1):64.
17 Vega MA, Simón-Fuentes M, González de la Aleja A, Nieto C, Colmenares M, Herrero C, et al. MAFB and MAF transcription factors as macrophage checkpoints for COVID-19 severity. Front Immunol. 2020;11:603507.
18 Cuevas VD, Anta L, Samaniego R, Orta-Zavalza E, Vladimir de la Rosa J, Baujat G, et al. MAFB determines human macrophage anti-inflammatory polarization: relevance for the pathogenic mechanisms operating in multicentric carpotarsal osteolysis. J Immunol. 2017;198(5):2070–81.
19 Kim H. The transcription factor MafB promotes anti-inflammatory M2 polarization and cholesterol efflux in macrophages. Sci Rep. 2017;7(1):7591.
20 Kang K, Park SH, Chen J, Qiao Y, Giannopoulou E, Berg K, et al. Interferon-γ represses M2 gene expression in human macrophages by disassembling enhancers bound by the transcription factor MAF. Immunity. 2017;47(2):235–e4.
21 Puig-Kröger A, Sierra-Filardi E, Domínguez-Soto A, Samaniego R, Corcuera MT, Gómez-Aguado F, et al. Folate receptor beta is expressed by tumor-associated macrophages and constitutes a marker for M2 anti-inflammatory/regulatory macrophages. Cancer Res. 2009;69(24):9395–403.
22 Liu M, Tong Z, Ding C, Luo F, Wu S, Wu C, et al. Transcription factor c-Maf is a checkpoint that programs macrophages in lung cancer. J Clin Invest. 2020;130(4):2081–96.
23 Joshi N, Watanabe S, Verma R, Jablonski RP, Chen CI, Cheresh P, et al. A spatially restricted fibrotic niche in pulmonary fibrosis is sustained by M-CSF/M-CSFR signalling in monocyte-derived alveolar macrophages. Eur Respir J. 2020;55(1):1900646.
24 Ushach I, Zlotnik A. Biological role of granulocyte macrophage colony-stimulating factor (GM-CSF) and macrophage colony-stimulating factor (M-CSF) on cells of the myeloid lineage. J Leukoc Biol. 2016;100(3):481–9.
25 Van Overmeire E, Stijlemans B, Heymann F, Keirsse J, Morias Y, Elkrim Y, et al. M-CSF and GM-CSF receptor signaling differentially regulate monocyte maturation and macrophage polarization in the tumor microenvironment. Cancer Res. 2016;76(1):35–42.
26 Murray PJ, Allen JE, Biswas SK, Fisher EA, Gilroy DW, Goerdt S, et al. Macrophage activation and polarization: nomenclature and experimental guidelines. Immunity. 2014;41(1):14–20.
27 Wynn TA, Chawla A, Pollard JW. Macrophage biology in development, homeostasis and disease. Nature. 2013;496(7446):445–55.
28 Hamilton JA. Colony-stimulating factors in inflammation and autoimmunity. Nat Rev Immunol. 2008;8(7):533–44.
29 Fleetwood AJ, Dinh H, Cook AD, Hertzog PJ, Hamilton JA. GM-CSF- and M-CSF-dependent macrophage phenotypes display differential dependence on type I interferon signaling. J Leukoc Biol. 2009;86(2):411–21.
30 Verreck FA, de Boer T, Langenberg DM, Hoeve MA, Kramer M, Vaisberg E, et al. Human IL-23-producing type 1 macrophages promote but IL-10-producing type 2 macrophages subvert immunity to (myco) bacteria. Proc Natl Acad Sci USA. 2004;101(13):4560–5.
31 Sierra-Filardi E, Puig-Kröger A, Blanco FJ, Nieto C, Bragado R, Palomero MI, et al. Activin A skews macrophage polarization by promoting a proinflammatory phenotype and inhibiting the acquisition of anti-inflammatory macrophage markers. Blood. 2011;117(19):5092–101.
32 Pyonteck SM, Akkari L, Schuhmacher AJ, Bowman RL, Sevenich L, Quail DF, et al. CSF-1R inhibition alters macrophage polarization and blocks glioma progression. Nat Med. 2013;19(10):1264–72.
33 Amemiya H, Kono H, Fujii H. Liver regeneration is impaired in macrophage colony stimulating factor deficient mice after partial hepatectomy: the role of M-CSF-induced macrophages. J Surg Res. 2011;165(1):59–67.
34 Kubota Y, Takubo K, Shimizu T, Ohno H, Kishi K, Shibuya M, et al. M-CSF inhibition selectively targets pathological angiogenesis and lymphangiogenesis. J Exp Med. 2009;206(5):1089–102.
35 Fleetwood AJ, Lawrence T, Hamilton JA, Cook AD. Granulocyte-macrophage colony-stimulating factor (CSF) and macrophage CSF-dependent macrophage phenotypes display differences in cytokine profiles and transcription factor activities: implications for CSF blockade in inflammation. J Immunol. 2007;178(8):5245–52.
36 Lacey DC, Achuthan A, Fleetwood AJ, Dinh H, Roiniotis J, Scholz GM, et al. Defining GM-CSF- and macrophage-CSF-dependent macrophage responses by in vitro models. J Immunol. 2012;188(11):5752–65.
37 Gonzalez-Dominguez E, Dominguez-Soto A, Nieto C, Luis Flores-Sevilla J, Pacheco-Blanco M, Campos-Pena V, et al. Atypical activin A and IL-10 production impairs human CD16 (+) monocyte differentiation into anti- inflammatory macrophages. J Immunol. 2016;196(3):1327–37.
38 Gonzalez-Dominguez E, Samaniego R, Flores-Sevilla JL, Campos-Campos SF, Gomez-Campos G, Salas A, et al. CD163L1 and CLEC5A discriminate subsets of human resident and inflammatory macrophages in vivo. J Leukoc Biol. 2015;98(4):453–66.
39 Palacios BSBS, Estrada-Capetillo L, Izquierdo E, Criado G, Nieto C, Municio C, et al. Macrophages from the synovium of active rheumatoid arthritis exhibit an activin a-dependent pro-inflammatory profile. J Pathol. 2015;235(3):515–26.
40 Schultze JL. Reprogramming of macrophages: new opportunities for therapeutic targeting. Curr Opin Pharmacol. 2016;26:10–5.
41 Riera-Borrull M, Cuevas VD, Alonso B, Vega MA, Joven J, Izquierdo E, et al. Palmitate conditions macrophages for enhanced responses toward inflammatory stimuli via JNK activation. J Immunol. 2017;199(11):3858–69.
42 Dominguez-Soto A, Sierra-Filardi E, Puig-Kroger A, Perez-Maceda B, Gomez-Aguado F, Corcuera MT, et al. Dendritic cell-specific ICAM-3-grabbing nonintegrin expression on M2-polarized and tumor-associated macrophages is macrophage-CSF dependent and enhanced by tumor-derived IL-6 and IL-10. J Immunol. 2011;186(4):2192–200.

43 Kuleshov MV, Jones MR, Rouillard AD, Fernandez NF, Duan Q, Wang Z, et al. Enrichr: a comprehensive gene set enrichment analysis web server 2016 update. Nucleic Acids Res. 2016;44(W1):W90–7.
44 Subramanian A, Tamayo P, Mootha VK, Mukherjee S, Ebert BL, Gillette MA, et al. Gene set enrichment analysis: a knowledge-based approach for interpreting genome-wide expression profiles. Proc Natl Acad Sci USA. 2005; 102(43):15545–50.
45 Langmead B, Salzberg SL. Fast gapped-read alignment with Bowtie 2. Nat Methods. 2012; 9(4):357–9.
46 Li B, Dewey CN. RSEM: accurate transcript quantification from RNA-Seq data with or without a reference genome. BMC Bioinformatics. 2011;12:323.
47 Yu G, Wang LG, Yan GR, He QY. DOSE: an R/ bioconductor package for disease ontology semantic and enrichment analysis. Bioinformatics. 2015;31(4):608–9.
48 Yu G, Wang LG, Han Y, He QY. ClusterProfiler: an R package for comparing biological themes among gene clusters. OMICS. 2012; 16(5):284–7.
49 Kawai T, Akira S. Toll-like receptors and their crosstalk with other innate receptors in infection and immunity. Immunity. 2011;34(5): 637–50.
50 Gabryšová L, Howes A, Saraiva M, O'Garra A. The regulation of IL-10 expression. Curr Top Microbiol Immunol. 2014;380:157–90.
51 Murray PJ. Understanding and exploiting the endogenous interleukin-10/STAT3-mediated anti-inflammatory response. Curr Opin Pharmacol. 2006;6(4):379–86.
52 Park JS, Svetkauskaite D, He Q, Kim JY, Strassheim D, Ishizaka A, et al. Involvement of toll-like receptors 2 and 4 in cellular activation by high mobility group box 1 protein. J Biol Chem. 2004;279(9):7370–7.
53 Lancaster GI, Langley KG, Berglund NA, Kammoun HL, Reibe S, Estevez E, et al. Evidence that TLR4 is not a receptor for saturated fatty acids but mediates lipid-induced inflammation by reprogramming macrophage metabolism. Cell Metab. 2018;27(5):1096–e5.
54 Xu G, Qi F, Li H, Yang Q, Wang H, Wang X, et al. The differential immune responses to COVID-19 in peripheral and lung revealed by single-cell RNA sequencing. Cell Discov. 2020 Dec;6(1):73.
55 Shaath H, Vishnubalaji R, Elkord E, Alajez NM. Single-cell transcriptome analysis highlights a role for neutrophils and inflammatory macrophages in the pathogenesis of severe COVID-19. Cells. 2020 Oct;9(11):2374.
56 Melms JC, Biermann J, Huang H, Wang Y, Nair A, Tagore S, et al. A molecular single-cell lung atlas of lethal COVID-19. Nature. 2021(7865): 595.
57 Xiong Y, Liu Y, Cao L, Wang D, Guo M, Jiang A, et al. Transcriptomic characteristics of bronchoalveolar lavage fluid and peripheral blood mononuclear cells in COVID-19 patients. Emerg Microbes Infect. 2020;9(1):761–70.
58 Cassetta L, Fragkogianni S, Sims AH, Swierczak A, Forrester LM, Zhang H, et al. Human tumor-associated macrophage and monocyte transcriptional landscapes reveal cancer-specific reprogramming, biomarkers, and therapeutic targets. Cancer Cell. 2019;35(4):588–e10.
59 Yarilina A, Park-Min KH, Antoniv T, Hu X, Ivashkiv LB. TNF activates an IRF1-dependent autocrine loop leading to sustained expression of chemokines and STAT1-dependent type I interferon-response genes. Nat Immunol. 2008;9(4):378–87.
60 Reynier F, de Vos AF, Hoogerwerf JJ, Bresser P, van der Zee JS, Paye M, et al. Gene expression profiles in alveolar macrophages induced by lipopolysaccharide in humans. Mol Med. 2012; 18:1303–11.
61 Li T, Fan J, Wang B, Traugh N, Chen Q, Liu JS, et al. TIMER: a web server for comprehensive analysis of tumor-infiltrating immune cells. Cancer Res. 2017;77(21):e108–10.
62 Cassetta L, Pollard JW. Targeting macrophages: therapeutic approaches in cancer. Nat Rev Drug Discov. 2018;17(12):887–904.
63 Cassetta L, Pollard JW. Repolarizing macrophages improves breast cancer therapy. Cell Res. 2017;27(8):963–4.
64 Sica A, Mantovani A. Macrophage plasticity and polarization: in vivo veritas. J Clin Invest. 2012;122(3):787–95.
65 Schultze JL, Freeman T, Hume DA, Latz E. A transcriptional perspective on human macrophage biology. Semin Immunol. 2015;27(1): 44–50.
66 Xue J, Schmidt SV, Sander J, Draffehn A, Krebs W, Quester I, et al. Transcriptome-based network analysis reveals a spectrum model of human macrophage activation. Immunity. 2014; 40(2):274–88.
67 Martinez FO, Gordon S, Locati M, Mantovani A. Transcriptional profiling of the human monocyte-to-macrophage differentiation and polarization: new molecules and patterns of gene expression. J Immunol. 2006;177(10): 7303–11.
68 McBerry C, Gonzalez RM, Shryock N, Dias A, Aliberti J. SOCS2-induced proteasome-dependent TRAF6 degradation: a common anti-inflammatory pathway for control of innate immune responses. PLoS One. 2012;7(6):e38384.
69 Zadjali F, Santana-Farre R, Vesterlund M, Carow B, Mirecki-Garrido M, Hernandez-Hernandez I, et al. SOCS2 deletion protects against hepatic steatosis but worsens insulin resistance in high-fat-diet-fed mice. Faseb J. 2012; 26(8):3282–91.
70 Machado FS, Esper L, Dias A, Madan R, Gu Y, Hildeman D, et al. Native and aspirin-triggered lipoxins control innate immunity by inducing proteasomal degradation of TRAF6. J Exp Med. 2008;205(5):1077–86.
71 Machado FS, Johndrow JE, Esper L, Dias A, Bafica A, Serhan CN, et al. Anti-inflammatory actions of lipoxin A4 and aspirin-triggered lipoxin are SOCS-2 dependent. Nat Med. 2006; 12(3):330–4.
72 Takenaka MC, Gabriely G, Rothhammer V, Mascanfroni ID, Wheeler MA, Chao CC, et al. Control of tumor-associated macrophages and T cells in glioblastoma via AHR and CD39. Nat Neurosci. 2019;22(5):729–40.
73 de Andres MC, Imagawa K, Hashimoto K, Gonzalez A, Goldring MB, Roach HI, et al. Suppressors of cytokine signalling (SOCS) are reduced in osteoarthritis. Biochem Biophys Res Commun. 2011;407(1):54–9.
74 Bromberg JS, Hittle L, Xiong Y, Saxena V, Smyth EM, Li L, et al. Gut microbiota-dependent modulation of innate immunity and lymph node remodeling affects cardiac allograft outcomes. JCI insight. 2018;3(19): e121045.
75 Hauser MA, Legler DF. Common and biased signaling pathways of the chemokine receptor CCR7 elicited by its ligands CCL19 and CCL21 in leukocytes. J Leukoc Biol. 2016;99(6):869–82.
76 Comerford I, Harata-Lee Y, Bunting MD, Gregor C, Kara EE, McColl SR. A myriad of functions and complex regulation of the CCR7/ CCL19/CCL21 chemokine axis in the adaptive immune system. Cytokine Growth Factor Rev. 2013;24(3):269–83.
77 Otero C, Groettrup M, Legler DF. Opposite fate of endocytosed CCR7 and its ligands: recycling versus degradation. J Immunol. 2006;177(4): 2314–23.
78 Bardi G, Lipp M, Baggiolini M, Loetscher P. The T cell chemokine receptor CCR7 is internalized on stimulation with ELC, but not with SLC. Eur J Immunol. 2001;31(11):3291–7.
79 Ouyang W, O'Garra A. IL-10 family cytokines IL-10 and IL-22: from basic science to clinical translation. Immunity. 2019;50(4):871–91.
80 Mumm JB, Emmerich J, Zhang X, Chan I, Wu L, Mauze S, et al. IL-10 elicits IFNγ-dependent tumor immune surveillance. Cancer Cell. 2011; 20(6):781–96.
81 Naing A, Infante JR, Papadopoulos KP, Chan IH, Shen C, Ratti NP, et al. PEGylated IL-10 (pegilodecakin) induces systemic immune activation, CD8+ T cell invigoration and polyclonal T cell expansion in cancer patients. Cancer Cell. 2018;34(5):775–e3.
82 Geginat J, Larghi P, Paroni M, Nizzoli G, Penatti A, Pagani M, et al. The light and the dark sides of Interleukin-10 in immune-mediated diseases and cancer. Cytokine Growth Factor Rev. 2016;30:87–93.
83 Bonelli S, Geeraerts X, Bolli E, Keirsse J, Kiss M, Pombo Antunes AR, et al. Beyond the M-CSF receptor: novel therapeutic targets in tumor-associated macrophages. FEBS J. 2018;285(4): 777–87.
84 Cannons JL, Tangye SG, Schwartzberg PL. SLAM family receptors and SAP adaptors in immunity. Annu Rev Immunol. 2011;29(1): 665–705.